BIOLOGY OF REPRODUCTION **71,** 117–129 (2004)
Published online before print 3 March 2004.
DOI 10.1095/biolreprod.103.027003

Structural and Functional Modifications of Sertoli Cells in the Testis of Adult Follicle-Stimulating Hormone Receptor Knockout Mice[1]

Amit Grover,[4,5] M. Ram Sairam,[2,4,5] Charles E. Smith,[3,6,7] and Louis Hermo[6]

Molecular Reproduction Research Laboratory,[4] Clinical Research Institute of Montreal, Montreal, Québec, Canada H2W 1R7
Department of Physiology,[5] McGill University, Montreal, Québec, Canada H3G 1Y6
Department of Anatomy and Cell Biology,[6] and Faculty of Dentistry,[7] McGill University, Montreal, Québec, Canada H3A 2B2

ABSTRACT

Follicle stimulating hormone (FSH) plays important roles during testicular development and in the maintenance of spermatogenesis in the adult. However, the cellular events or pathways that FSH regulates to achieve these effects in Sertoli cells, where the FSH receptors (FSH-R) are located, is still not fully elucidated. The development of FSH-R knockout (FORKO) mice provides a model to examine alterations in testicular structure and function in its absence. To this end, light (LM) and electron microscopic (EM) analyses of perfusion-fixed testes of wild-type and FORKO mice of different ages were performed. Under the LM, a significant reduction was noted in the profile area of seminiferous tubules of FORKO mice compared with their wild-type counterparts at different ages. In addition, FORKO testes revealed large irregularly shaped spaces within the seminiferous epithelium, extending from the base to the lumen. Such spaces were often separated by anastomotic cords of spherical germ cells or completely surrounded elongating spermatids. This phenotype was restricted to half or less of the circumference of only some tubules, but was seen at all stages. EM analyses revealed that the spaces corresponded to an apparent accumulation of fluid in the Sertoli cell cytoplasm, coincident with an absence of the fine flocculent ground substance seen in wild-type mice. However, the Sertoli organelles, while less prominent, appeared intact and to be floating in the enlarged fluid-filled cytoplasm. Functionally, androgen-binding protein (ABP), a major secretory protein of Sertoli cells, was dramatically reduced in FORKO mice. These results suggest that FSH-R signaling normally maintains water balance in Sertoli cells in addition to regulating ABP production.

follicle-stimulating hormone receptor, male reproductive tract, Sertoli cells, sperm, testis

INTRODUCTION

Follicle stimulating hormone (FSH), a heterodimeric pituitary glycoprotein hormone considered essential for mammalian fertility, interacts specifically with its cognate receptor (FSH-R) localized in Sertoli and ovarian granulosa cells. The FSH-R, derived from a single gene, is produced as a Gs-protein coupled, seven-transmembrane receptor, which activates several signaling pathways to integrate target cellular activities [1–3]. In the testis, FSH has a differential effect on Sertoli cells in accordance with the different stages of the cycle of the seminiferous epithelium. While the hormone is maximally bound at stage I [4, 5], FSH stimulated cAMP production peaks at stage IV, with cAMP responsive element binding protein (CREB) mRNA levels peaking at stage VII of the cycle [6, 7]. In the adult testis, the nondividing population of Sertoli cells performs diverse functions. In addition to anchoring and nourishing germ cells, they form the blood testis barrier, phagocytose residual bodies, release sperm at the time of spermiation, and participate in secretion and endocytosis of various substances, including ions and proteins [8–11].

Also important is the fact that Sertoli cells transport water from the interstitial space into the lumen, serving as the vehicle for moving sperm from the testis to the epididymis [12, 13]. In addition to basolaterally located ion channels, recent studies have revealed that aquaporins (water channels) are abundant in the testis, with some being localized to Sertoli cells [14–16]. Interestingly, various members of the aquaporin gene family contain CRE motifs (CREB binding regions) and are under cAMP regulation [17–20], a second messenger that is activated upon FSH-R signaling [1]. In the testis, Jegou et al. [21] first demonstrated a selective action of FSH, proposing that this hormone is involved in fluid absorption/secretion; however, the cell type involved or the mechanism of action was not evaluated.

In addition to fluid regulation, Sertoli cells are responsible for the secretion of numerous proteins into the seminiferous tubular lumen, such as the glycoprotein androgen binding protein (ABP). ABP binds androgens with high affinity and transports them to the epididymis [22–24]. Regulation of ABP by FSH and testosterone has been demonstrated [25], although whether one or both are required for complete function remains to be resolved [22]. ABP also displays a stage-specific expression pattern within the seminiferous epithelium and its secretion has often been regarded as an index of Sertoli cell function [22, 26]. Recent work with transgenic mice overexpressing rat ABP has shed more light on the role of ABP in spermatogenesis. The predominant phenotypic anomaly observed in these mice is a decrease in fertility, suggesting that altered levels of ABP are in fact associated with impaired fertility [22, 27, 28].

While Sertoli cells respond to FSH stimulation, the na-

[1]This study was funded by grants from the CIHR (M.R.S. and L.H.).
[2]Correspondence: M. Ram Sairam, Molecular Reproduction Research Laboratory, Clinical Research Institute of Montreal, 110 Avenue des Pins West, Montréal, Québec, Canada H2W 1R7. FAX: 514 987 5585; e-mail: sairamm@ircm.qc.ca
[3]Current address: Faculte de Medecine Dentaire, Universite de Montreal, Québec, Canada H3C 3J7.

Received: 23 December 2003.
First decision: 20 January 2004.
Accepted: 19 February 2004.

ISSN: 0006-3363. http://www.biolreprod.org

ture of the response itself varies depending on the developmental status of the animal. Early studies demonstrated that FSH acts as a Sertoli cell mitogen in the prenatal and newborn animal and is instrumental in determining the final spermatogenic capability of the testis [29]. In immature mice, it has been shown that FSH-R signaling appears to be essential for testicular development, the initiation of the first wave of spermatogenesis, and sexual maturity [30, 31]. The critical role played by FSH/FSH-R signaling has been further illustrated through newly uncovered human mutations in the FSHβ subunit [32–35]. Such men display hypogonadism, obstructed pubertal development, small testis size, and azoospermia [32–34]. Interestingly, mice that lack the FSHβ subunit [35] are fertile, as are some Finnish men with an inactivating FSH-R mutation [36]. In both these examples, testis size and sperm production levels are reduced [35, 36].

The development of mice deficient in the FSH receptor (FORKO) provides a model to examine alterations in testicular structure and function in its complete absence [37]. Mutant mice at 2 mo of age have smaller testes, delayed sexual maturity, and reduced fertility [30, 37, 38]. In addition, serum FSH levels are elevated [37] and testosterone levels are reduced [37–39] amid normal circulating levels of LH [39]. However, details on the structure and functions of the cell type(s) affected in the testis of FORKO mice at early and later ages have not been studied in any detail. This investigation was designed to shed more light on the structural alterations in Sertoli cells of the mutants and their potential impact on functions.

MATERIALS AND METHODS

Animals

This investigation was approved by the ethics committee of the Clinical Institute of Montreal and McGill University and was conducted according to accepted standards of animal experimentation. The FORKO mice were generated by homologous recombination as described by Dierich et al. [37]. This alteration eliminates the entire repertoire of FSH-R forms, producing complete loss of hormone signaling. Breeding F2 heterozygous males and females produced mice of all three genotypes in the SV129 background. The animals were maintained under well-controlled conditions of temperature (22°C) and light (12L:12D), with food and water provided ad libitum. The primers and amplification conditions used for the multiplex polymerase chain reaction (PCR) to identify the phenotypes have been described in detail elsewhere [40]. According to this protocol, a single PCR performed on each sample allowed unambiguous identification of +/+, +/−, and −/− mice.

Routine Light and Electron Microscopic Methods

A total of 16 mice at 3 and 6 mo of age (wild type, n = 4; FORKO, n = 4, for each age group) were used for detailed ultrastructural analyses of their testes. The mice were anesthetized by an intraperitoneal injection with sodium pentobarbital (Somnitol; MTC Pharmaceuticals, Hamilton, ON, Canada). Prior to perfusion, a hemostat was placed over the testicular vessels entering the left testis of each animal; this testis was removed, immersed in Bouin fixative and, after 10 min, cut in half and left in Bouin for 24 h. Thereafter, all the left testes were dehydrated in alcohol and subsequently embedded in paraffin.

The remaining right testis of each animal was kept intact and immediately fixed by cardiac perfusion with 2.5% or 5% glutaraldehyde buffered in sodium cacodylate (0.1 M) containing 0.05% calcium chloride (pH 7.4). After 10 min of perfusion, the right testes were removed from the scrotum, cut into small 1-mm cubes and placed in the same fixative for an additional 2 h at 4°C. Thereafter, the tissues were thoroughly rinsed three times in 0.1 M sodium cacodylate buffer containing 0.2 M sucrose and left in this buffer overnight. On the following day, the testes were postfixed in ferrocyanide-reduced osmium tetroxide for 1 h at 4°C, dehydrated in a graded series of ethanol and propylene oxide, and embedded in Epon. Thick sections (0.5 μm) were cut with glass knives and stained with toluidine blue and observed by light microscopy. Thin sections (gray to silver interference color) of selected regions of each block were cut with a diamond knife, placed on copper grids, and counterstained with uranyl acetate (5 min) and lead citrate (2 min). Sections were examined with a Philips 400 electron microscope (Phillips, Eindhoven, The Netherlands).

Quantitative Analyses

The left testes from the 3- and 6-mo-old wild-type and FORKO mice that had been fixed in Bouin fluid were utilized for quantitative analyses, along with other testes obtained from 12-mo-old wild-type (n = 4) and FORKO (n = 4) mice that had been prepared and fixed in Bouin fluid for a different study. Scaled digital images of 5-μm-thick paraffin sections of seminiferous tubules from these animals were captured on a Zeiss Axioscop 2 equipped with an AxiocamMR camera, and the peripheral outline of selected tubules was traced and the profile areas determined using the appropriate measurement tool available in Version 3.1 of the Axiovision Imaging Software (Carl Zeiss Canada Ltd., Montreal, QC). In all cases, only those seminiferous tubules showing a near-perfect transverse plane of section were measured, and a minimum of 150 tubular cross-sectional profiles were outlined in sections from animals of a given age and treatment group. Preliminary analyses of the data indicated that profile areas of the seminiferous tubules were not distributed along a normal curve in either the wild-type or the FORKO mice, and $\log_{10}$ transformations of raw data had to be done in order to obtain normal distributions. These transformations and subsequent univariate factorial ANOVA test and post hoc unequal N HSD *t*-tests were done using Version 6.1 of STATISTICA for Windows (Statsoft, Inc., Tulsa, OK); P values < 0.05 were considered significant.

LM Immunocytochemistry

The following affinity-purified polyclonal antibodies were used at 1:100 dilution (v/v) for routine peroxidase immunostaining: 1) antiprosaposin antibody (provided by Dr. C.R. Morales, McGill University, Montreal, Canada; purified and characterized as described previously [41]) and 2) rabbit anti-ABP antibody prepared against a glutathione sulfo transferase (GST)-ABP fusion protein [42] (provided by Dr. G.L. Hammond, University of Western Ontario, London, Canada).

For the antiprosaposin antibody, 5-μm-thick paraffin sections of Bouin fixed testes were deparaffinized in Histoclear (Diamed Lab Supplies Inc., Mississauga, ON, Canada) and hydrated through a series of graded ethanol solutions. During hydration, residual picric acid was neutralized in 70% ethanol containing 1% lithium carbonate, and endogenous peroxidase activity was abolished by treating the sections with 70% ethanol containing 1% (v/v) H_2O_2. Once hydrated, the sections were washed in distilled water containing glycine to block free aldehyde groups. Nonspecific binding sites were blocked using 10% goat serum for 30 min. The sections were then incubated at 37°C in a humidified chamber for 90 min with 100 μl of primary antibody diluted in Tris-buffered saline (TBS). Following washes in 0.1% Tween20 in TBS, the slides were incubated with secondary antibody (1:250; 100 μl) labeled with horseradish peroxidase for 30 min at 37°C in a humidified chamber. Reactions were revealed with diaminobenzidine tetrahydrochloride (DAB). Sections were counterstained with methylene blue, dehydrated in ethanol and Histoclear, and mounted with cover slips using Permount. TBS substitution for primary antibody was used as a negative control. No reactions were observed in these sections.

For the anti-ABP antibody, paraffin sections were processed for immunostaining using the ImmunoCruz ABC Staining System (Santa Cruz Biotechnology Inc., Santa Cruz, CA). The sections were deparaffinized and hydrated as described above. Sections then were microwaved for antigen retrieval in citrate buffer [43]. After boiling and cooling, the ImmunoCruz system was employed as per the suppliers' instructions. Sections were incubated with the anti-ABP antibody at a dilution of 1:100 overnight at 4°C. The sections were then washed in phosphate buffered saline (PBS) and incubated in biotinylated secondary antibody (1:250) for 30 min at room temperature. Sections were washed again in PBS and incubated in an avidin-biotin-horseradish peroxidase solution for 30 min at room temperature. Reactions were visualized by DAB. The sections were counterstained with methylene blue, dehydrated, and mounted with cover slips. For negative controls, normal blocking serum was substituted for primary antibody; no reactions were detected in the epithelium.

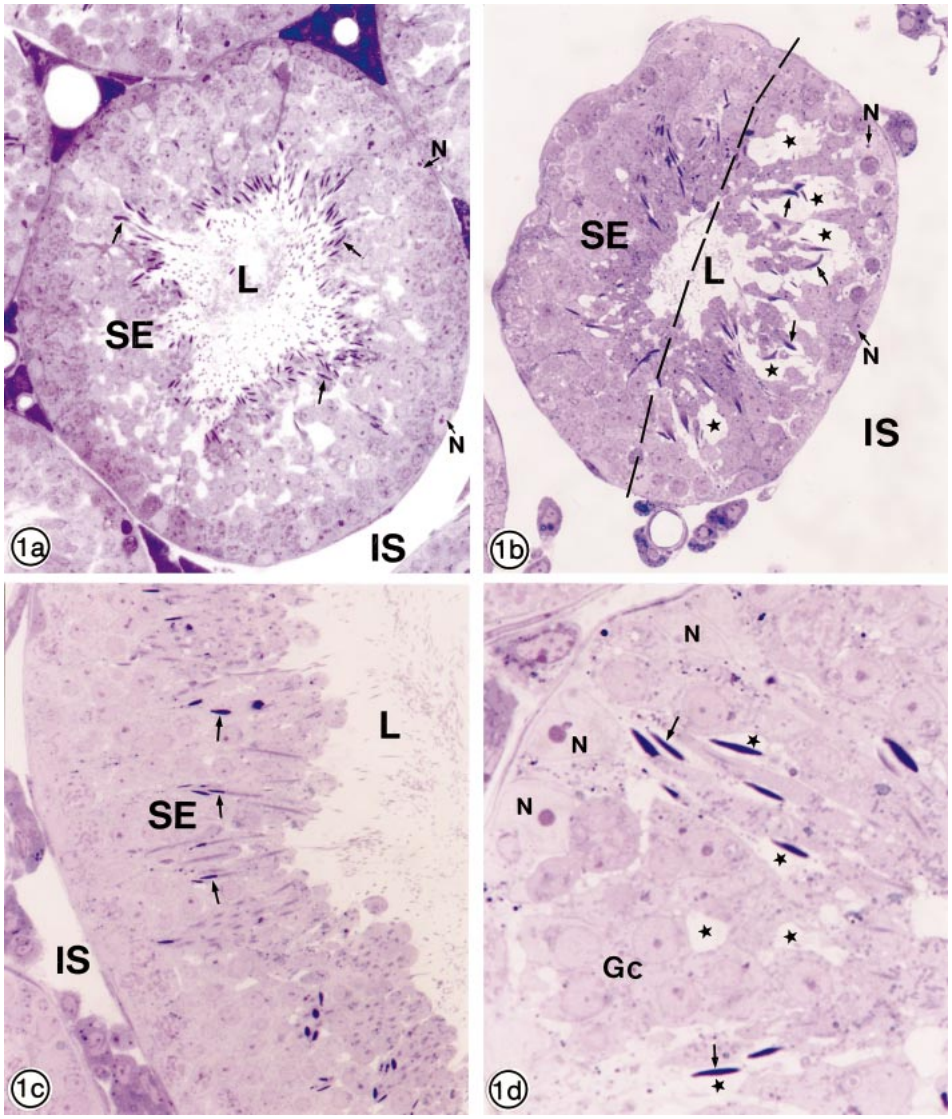

FIG. 1. Light micrographs of seminiferous tubules of the testis of wild-type (**a**, **c**) and FORKO (**b**, **d**) mice at 3 mo of age. Note reduction in size of the tubules of FORKO mice (**b**) as compared with their wild-type counterparts (**a**). In **a** and **c**, the seminiferous epithelium (SE) shows a close association of Sertoli cells with germ cells. The heads of the elongating spermatids (arrows) are tightly apposed to the enveloping Sertoli cells in wild-type mice (**a**, **c**). In contrast, in **b** and **d**, large empty spaces appear in the epithelium (stars), which tend on the whole to be localized to half the circumference of the affected tubules. Note that the dilated spaces (stars) in the midregion of the epithelium surround the heads of elongating spermatids (arrows). Gc, Germ cells; N, nucleus of Sertoli cell; IS, interstitial space; L, lumen. **a**, **b**) Original magnification ×250; (**c**) original magnification ×390; (**d**) original magnification ×1000.

Western Blot Analysis

A total of 6 mice at 6 mo of age (wild type, n = 3; FORKO, n = 3) were used for Western blot analysis. One testis of each mouse was extracted and cut into four equal pieces. Each piece was then frozen in liquid nitrogen for subsequent protein extraction. The frozen pieces of testis were homogenized, suspended in lysis buffer containing detergent and a protease inhibitor cocktail [39], and the solution was centrifuged at 11 000 × *g* for 15 min at 4°C. The supernatant was removed and quantified for protein using the Bradford Assay (Bio-Rad Laboratories Inc., Richmond, CA). Equivalent amounts of solubilized protein (30 μg) in SDS sample loading buffer were boiled for 5 min and electrophoresed on a 10% SDS polyacrylamide gel. Subsequently, the proteins were transferred onto nitrocellulose membranes for immunoblotting. Following incubation with the anti-ABP antibody at 1:500 (v/v) dilution and secondary antibody conjugated to horseradish peroxidase (1:1000 v/v), bands were revealed by chemiluminescence using the Pierce SuperSignal Western Blotting Kit (Pierce, Rockford, IL). Molecular weight markers were used to estimate the mass of the detected bands. The experiment was repeated a minimum of three times in duplicate. Equal protein loading was confirmed by Coomassie staining. Quantitative analysis of Western blot was performed using Chemi-Imager 4.0 software (B&L Systems, Maarssen, The Netherlands), which measured the spot density of each protein band on the exposed film. Raw density data was subject to an unpaired sample *t*-test; P values < 0.05 were considered significant.

RESULTS

Light Microscopic Appearance of the Testis of FORKO Mice

At 3 and 6 mo of age, the seminiferous tubules in the testis of FORKO mice showed smaller profile areas compared with wild-type mice (Fig. 1, a and b). In addition, while the testis of wild-type mice displayed a homogenous, compact seminiferous epithelium, where germ and Sertoli cells were closely associated with each other (Fig. 1, a and c), the FORKO mice presented a varying and vacuolated appearance (Figs. 1, b and d, and 2, a and b). Although some tubules at both ages seemed normal in cross-sectional profile (approximately 40%), nearly one half of the circumference of seminiferous epithelium of other tubules in the FORKO mice appeared disrupted, showing large dilated spaces between the epithelial cells (Figs. 1, b and d, and 2, a and b). This semilunar disruption pattern did not appear to be associated with a specific stage of the cycle of the seminiferous epithelium (Figs. 1, b and d, and 2, a and b).

In areas where the FORKO tubules were abnormal, large dilated spaces often extended from the base of the epithelium toward the lumen, and at the base, these spaces at

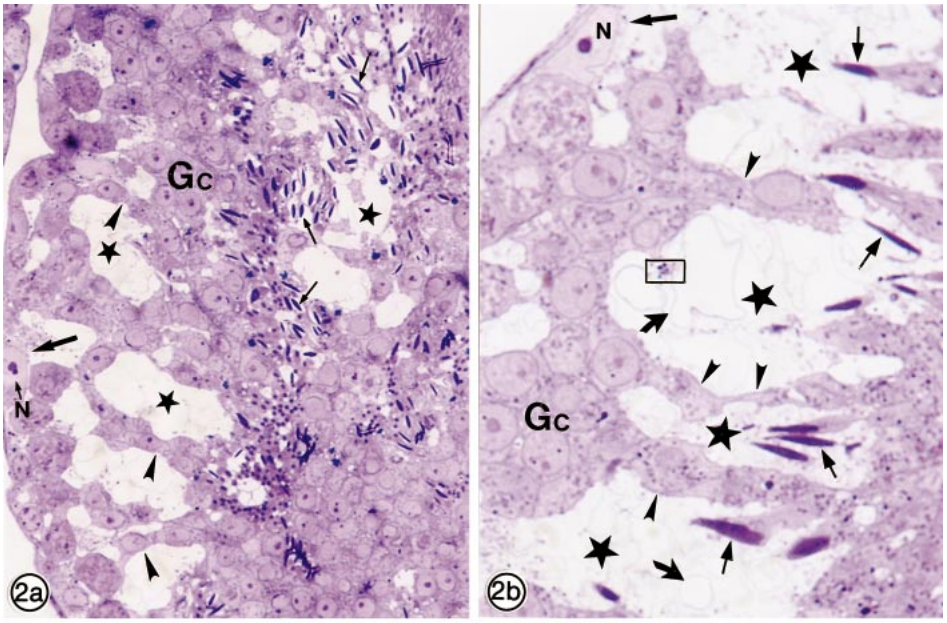

FIG. 2. Low (**a**) and high (**b**) power light micrographs of seminiferous tubules of FORKO mice at 6 mo of age. In **a** and **b**, the highly dilated translucent spaces (stars) are situated basally in the epithelium, with some enveloping the heads of elongating spermatids (thin arrows). In **a** and **b**, some spaces (thick arrows) are confluent with areas containing the Sertoli nucleus (N). The extensive nature of the dilated spaces gives rise to anastomotic cords (arrowheads) of spherical germ cells (Gc), which themselves do not appear to be dilated. Despite the extensive epithelial dilatations, there is no suggestion of pyknosis in the nuclei of Sertoli cells or of apoptotic cells. In the dilated spaces, numerous membranous profiles of varying sizes and shapes (curved arrows) are evident, as well as small particulate and granular material (square). **a**) Original magnification ×390; (**b**) original magnification ×1000.

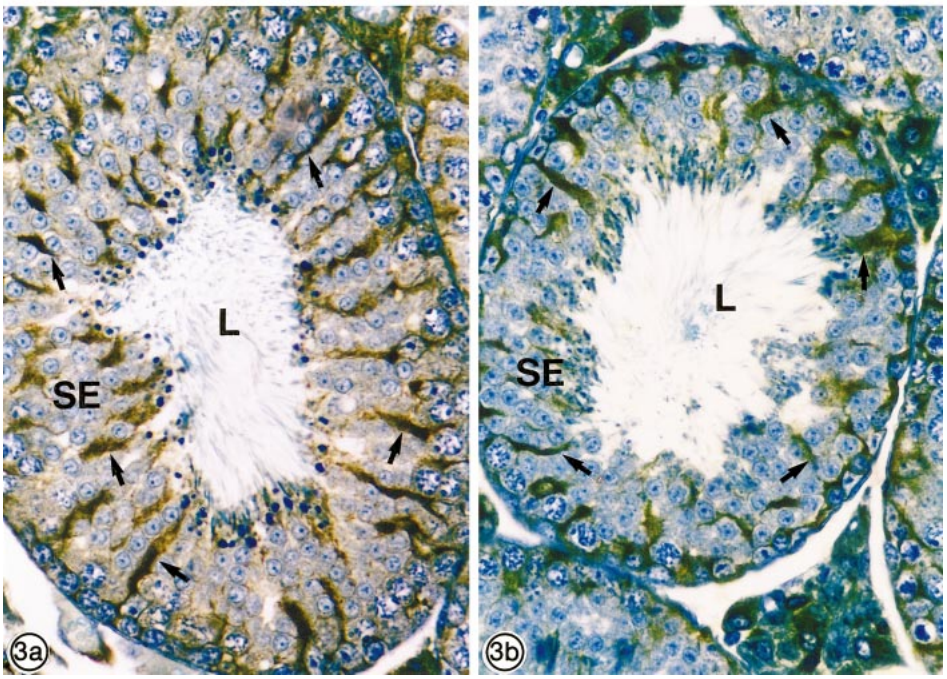

FIG. 3. Light micrographs of seminiferous tubules of 3-mo-old wild-type (**a**) and FORKO (**b**) mice immunostained with antiprosaposin antibody. Note reduction in the profile area of the tubules between wild-type and FORKO mice. Sertoli cells (arrows) are highly reactive and extend from the base of the seminiferous epithelium (SE) to the lumen (L) in both **a** and **b**; germ cells are unreactive. **a**, **b**) Original magnification ×390.

times hovered over the nuclei of Sertoli cells (Fig. 2, a and b). In the midregion of the epithelium, the dilated spaces often separated chains of round spermatids from each other. In this way, they formed cords or ribbons, which gave the epithelium an anastomotic appearance due to their extensive nature (Fig. 2, a and b). The large dilated spaces of varying sizes also surrounded elongating spermatids, which they often completely enveloped (Figs. 1, b and d, and 2, a and b). The interior of the dilated spaces often contained membranous profiles of varying sizes and spherical particulate material (Fig. 2b). The various generations of germ cells did not display any signs of structural abnormalities or spaces in their cytoplasm (Figs. 1, b and d, and 2, a and b). In the interstitial spaces of FORKO mice that seemed to be enlarged, Leydig cells, macrophages, and blood vessels were structurally similar in appearance to those seen in the wild-type mice. There was no evidence of any increase in macrophage number or infiltration of neutrophils in the interstitial spaces of FORKO mice.

Immunocytochemical Analyses

Antiprosaposin antibody revealed Sertoli cells spanning the circumference of each tubule in a regular and spokelike manner (Fig. 3, a and b). The staining pattern radiated from the base of the epithelium toward the lumen over a distance that appeared shorter in the FORKO mice due to the smaller profile areas of tubules in these animals compared with wild-type mice (Fig. 3, a and b).

An intense anti-androgen binding protein (ABP) reaction was noted over the cytoplasm of Sertoli cells at all stages of the cycle of the seminiferous epithelium of wild-type mice; the reaction extended from the base of the epithelium to the lumen (Fig. 4, a, c, and e). No staining was observed

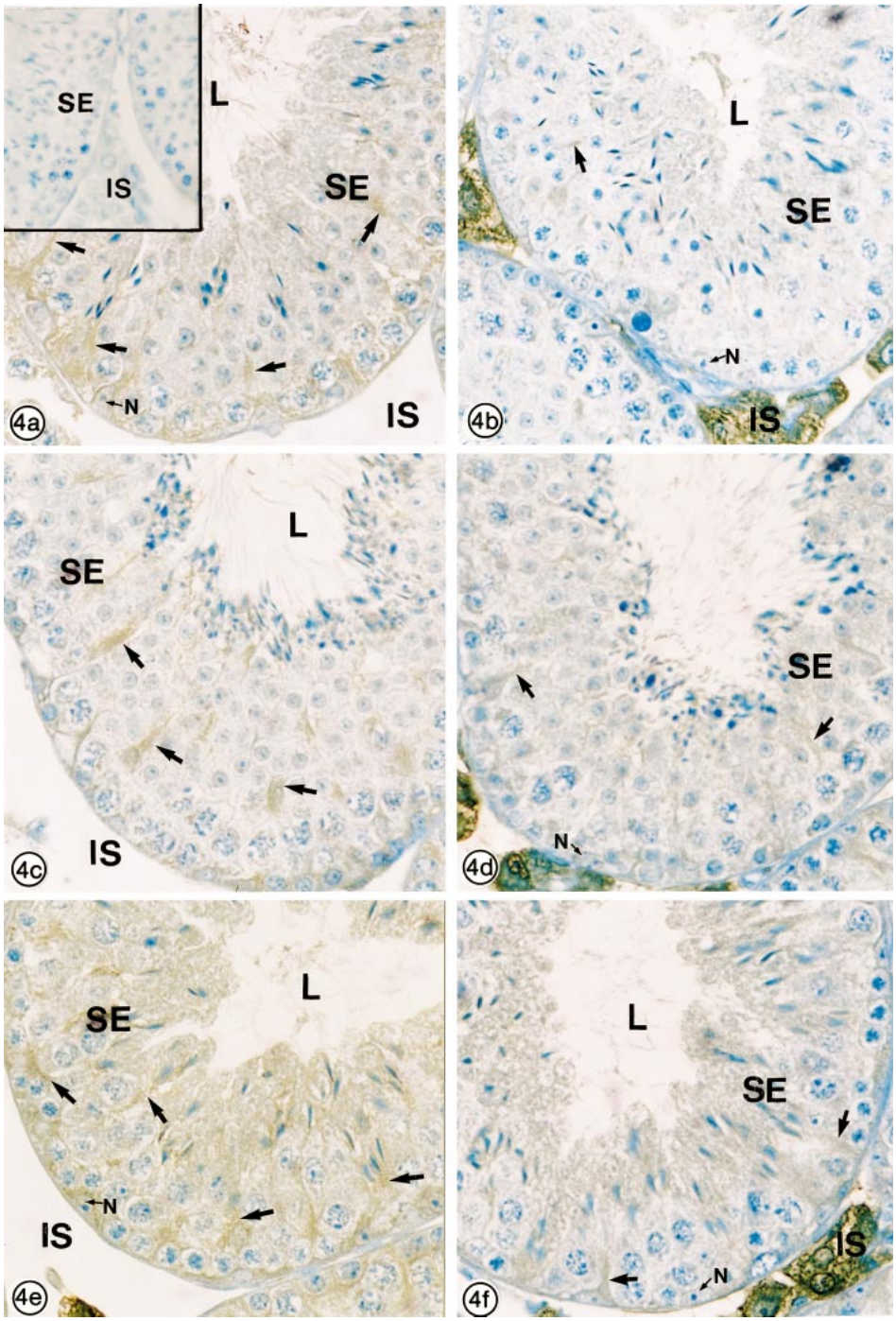

FIG. 4. Light micrographs of seminiferous tubules of wild-type (**a**, **c**, **e**) and FORKO (**b**, **d**, **f**) mice at 3 mo of age immunostained with an anti-ABP antibody. In wild-type mice at early (**a**, stage II–III), mid (**c**, stage VII), and late (**e**, stage XII) stages of the cycle, a reaction is evident in Sertoli cells, either basally or as distinct bands radiating across the width of the epithelium (arrows). This is in contrast to the weak staining or absence of a reaction over Sertoli cells of FORKO mice (arrows), seen at stages I (**b**), VII (**d**), and XII (**f**). The reaction over Leydig cells in the interstitial space (IS) is nonspecific. SE, Seminiferous epithelium; L, lumen; N, nucleus of Sertoli cell. **a**–**f**) Original magnification ×390; inset in **a**, original magnification ×250.

over germ cells. In FORKO mice, the staining over Sertoli cells at all stages of the cycle appeared weak and in some areas completely missing (Fig. 4, b, d, and f). A nonspecific staining of Leydig cells was evident in the interstitial spaces inherent to the anti-ABP protein construct (see *Materials and Methods*), and the fact that Leydig cells express GSTs [44]. Control sections showed no staining over the epithelium (Fig. 4a, inset).

Electron Microscopic Appearance of the Testis of FORKO Mice

While the nucleus of the affected Sertoli cells in FORKO mice was intact, showing a pale-stained uncondensed chromatin pattern and conspicuous nucleolus and satellite bodies as seen in wild-type mice (Fig. 5a), their cytoplasm was grossly disrupted; this was especially evident in the mid and apical areas of their cytoplasm (Figs. 5b, 6, 7b, and 8). In wild-type mice, the organelles in the expansive Sertoli cell cytoplasm were embedded in a compact, finely flocculent ground substance, with adjacent Sertoli cells being tethered together by a conspicuous Sertoli-Sertoli blood testis barrier (Fig. 5a). Sertoli and germ cells were closely associated with each other, with very small intercellular spaces positioned between the two. However, in FORKO mice, the seminiferous epithelium showed large dilated spaces surrounding nearby germ cells (Figs. 5b and 6). The basal Sertoli cell cytoplasm contacted the basement membrane and displayed various organelles such as lysosomes, mitochondria, endoplasmic reticulum (ER), and the Golgi

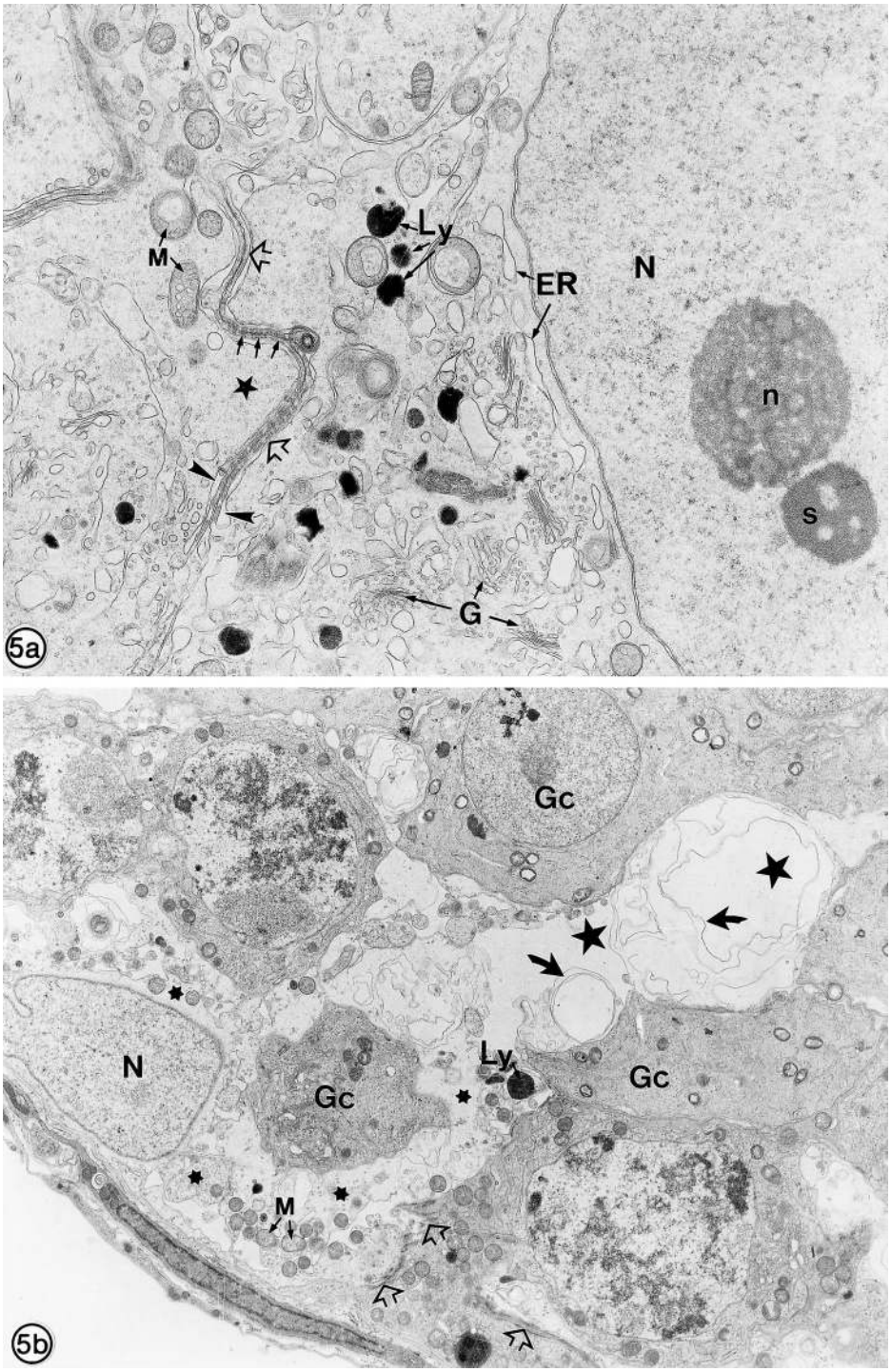

FIG. 5. Electron micrographs of the base of the seminiferous epithelium of wild-type (**a**) and FORKO mice at 3 mo of age (**b**). In **a**, organelles in the Sertoli cell cytoplasm, such as Golgi apparatus (G), lysosomes (Ly), mitochondria (M), and endoplasmic reticulum (ER), are embedded in a finely flocculent ground substance (star). The Sertoli-Sertoli blood testis barrier (open arrows) is intact and composed of bundles of filaments (small arrows) overlaid by flattened cisternae of endoplasmic reticulum (arrowheads). The Sertoli cell nucleus (N) is pale stained and shows a prominent nucleolus (n) and closely associated satellite body (s) in this plane of section. In **b**, the Sertoli cell cytoplasm is dilated in the midarea of the seminiferous epithelium (stars), where large membranous whorls are evident (curved arrows). Nearer to the base of the epithelium, the Sertoli cytoplasm shows small territories enclosing spherical mitochondria (M), lysosomes (Ly), and a pale stained nucleus (N), all embedded in a finely flocculent ground substance (asterisks). The large dilated Sertoli cytoplasm surrounds spherical germ cells (Gc) that do not show any structural abnormalities. **a**) Original magnification ×14 000; (**b**) original magnification ×6600.

apparatus, embedded in a finely flocculent ground substance (Figs. 5b and 6). However, large dilated spaces not connected to basal areas of Sertoli cell cytoplasm, due to the plane of section, were often observed in mid and apical regions of the epithelium (Fig. 5b). The fact that these dilated spaces were delimited by a plasma membrane and contained organelles indicated that they were territories of cytoplasm. Indeed, in appropriate planes of section, the large, dilated membrane-bound spaces were confluent with the intact basal areas of Sertoli cell cytoplasm (Fig. 6). It was thus concluded that the large, dilated spaces corresponded to extensive dilations of the Sertoli cell cytoplasm. In contrast, the cytoplasm of the neighboring spermatocytes or early round spermatids was not disrupted, and on no occasion did it ever appear dilated (Figs. 5b and 6). In the intact basal areas of the Sertoli cell cytoplasm, the Sertoli-Sertoli blood testis barrier of FORKO mice appeared to be intact. As in wild-type mice (Fig. 5a), bundles of filaments and ER cisternae closely approximated the expansive areas of tight junctions between the plasma membranes of adjacent Sertoli cells (Figs. 5b and 6).

In the mid and apical regions of the seminiferous epithelium of wild-type mice, the heads of elongating spermatids were deeply embedded in niches of Sertoli cell processes (Fig. 7a). The cytoplasm of the latter contained mitochondria, lysosomes, and ER cisternae, all embedded in

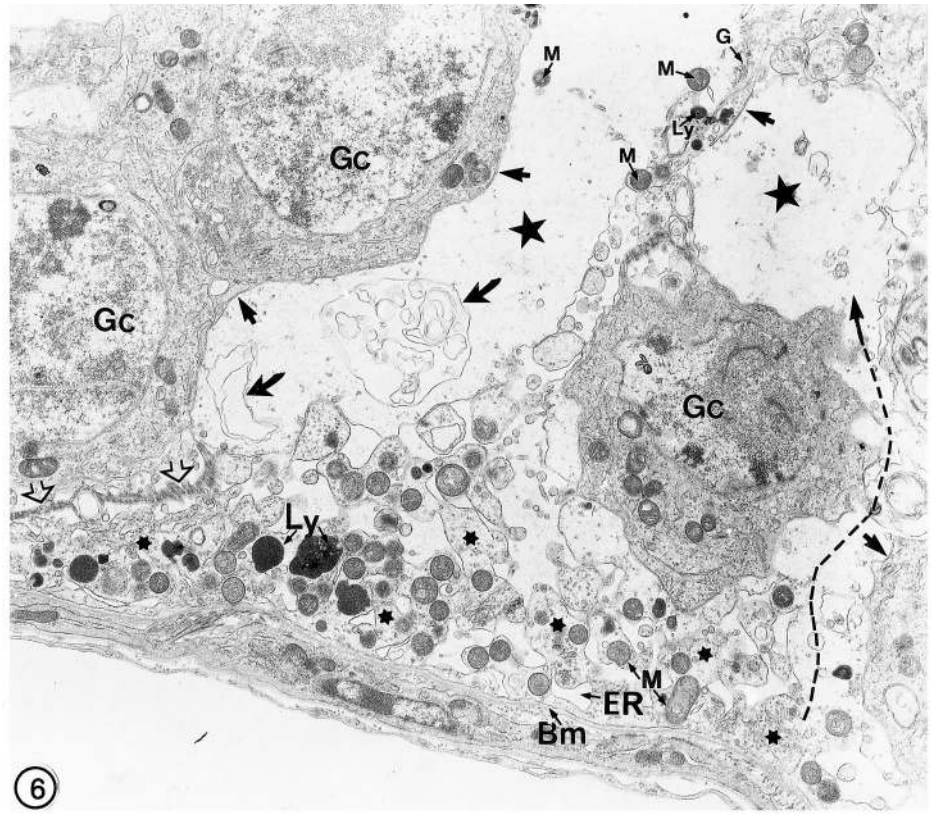

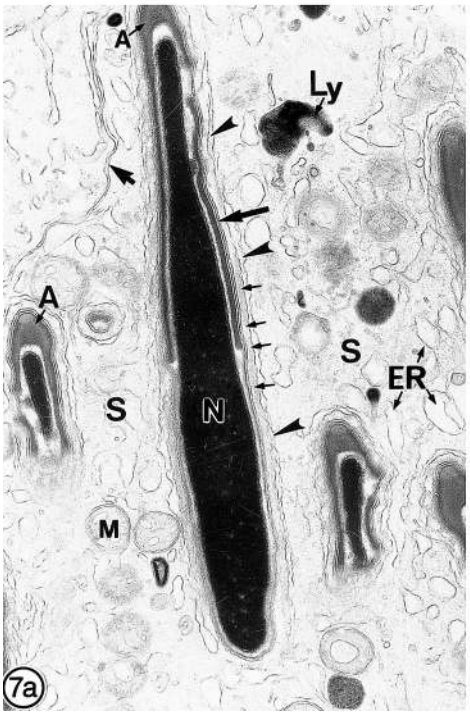

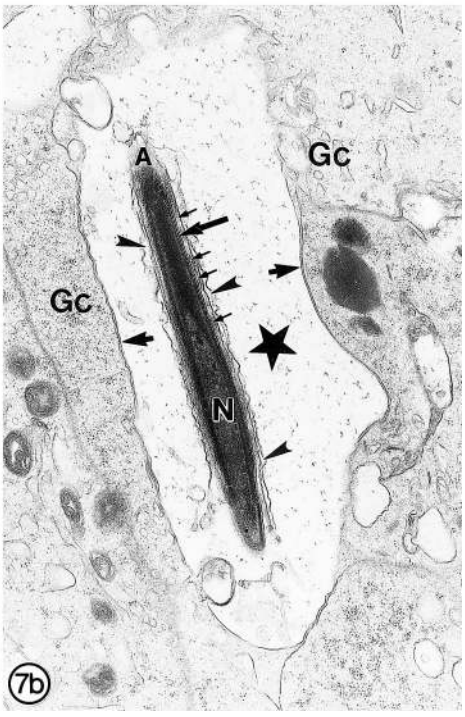

FIGS. 6 and 7. FIG. 6. Electron micrograph of the base and midregion of the seminiferous epithelium of a 6-mo-old FORKO mouse. Areas of Sertoli cell cytoplasm (asterisks) located basally are in contact with the basement membrane (Bm) and contain mitochondria (M), lysosomes (Ly), and cisternae of endoplasmic reticulum (ER), embedded in a finely flocculent ground substance. In the midregion of the epithelium, a large dilation of Sertoli cell cytoplasm (star), containing large membranous profiles (curved arrows), is separated from the basal cytoplasm of Sertoli cell cytoplasm presumably due to the plane of section. In the upper right hand corner of this dilation, mitochondria (M), a Golgi apparatus (G), and lysosomes (Ly) are evident, with two mitochondria (M) appearing to be floating freely in the interior of this dilation. Another large dilated space (long dashed arrow) extending toward the lumen appears to be confluent with the basal area of Sertoli cell cytoplasm containing intact organelles and ground substance. As both dilated spaces contain organelles and are delimited by a plasma membrane (arrows), they are considered to be dilations of the Sertoli cell cytoplasm and not extensions of the lumen. The Sertoli-Sertoli blood testis barrier at the base of the epithelium is evident and appears intact (open arrows). Germ cells (Gc) do not show any apparent structural abnormalities of their cytoplasm, nucleus, or organelles, and the organelles of the Sertoli cell themselves appear intact. Original magnification ×8600. FIG. 7. Heads of elongating spermatids enveloped by Sertoli cell processes in wild-type (**a**) and FORKO (**b**) mice at 3 mo of age. In **a**, the cytoplasm of the Sertoli cell processes (S) enveloping the spermatid head contains mitochondria (M), lysosomes (Ly), and ER, embedded in a finely flocculent ground substance. The ectoplasmic specializations, comprised of thick bundles of filaments (small arrows) and overlying flattened ER cisternae (arrowheads), are closely applied to the spermatid head. In **b**, the Sertoli cell process enveloping the spermatid head is greatly dilated and appears predominately organelle free (star). The ectoplasmic specialization adhering to the spermatid head appears to be less extensive, showing fewer bundles of filaments (small arrows) and at times dilated ER cisternae (arrowheads). However, the plasma membrane of the Sertoli cell process is closely apposed to the spermatid head (long arrows) and to that applied to the elongating germ cell (Gc) cytoplasm (short arrows). A, Acrosomes of spermatid head; N, nucleus of spermatid heads. (**a**) Original magnification ×16 100; (**b**) original magnification ×16 800.

a finely flocculent ground substance. In addition, bundles of filaments overlaid by ER cisternae, and forming the so-called ectoplasmic specializations, were closely applied to the spermatid heads (Fig. 7a). In the semilunar affected areas of the seminiferous epithelium of FORKO mice, a gross enlargement and dilation of the apical Sertoli cell cytoplasm was evident (Fig. 7b). In some planes of section, the dilated apical Sertoli cell processes, of enormous sizes, contained few organelles other than membranous profiles of various sizes (Fig. 8a). However, in other cases, such processes contained numerous organelles such as mitochondria, ER cisternae, lysosomes, and small vesicular profiles (Fig. 8b). The ectoplasmic specializations of the Sertoli cell processes also appeared to be affected. They showed fewer filaments and occasional swellings of their ER cisternae (Fig. 8, a and b). The dilated processes did not ap-

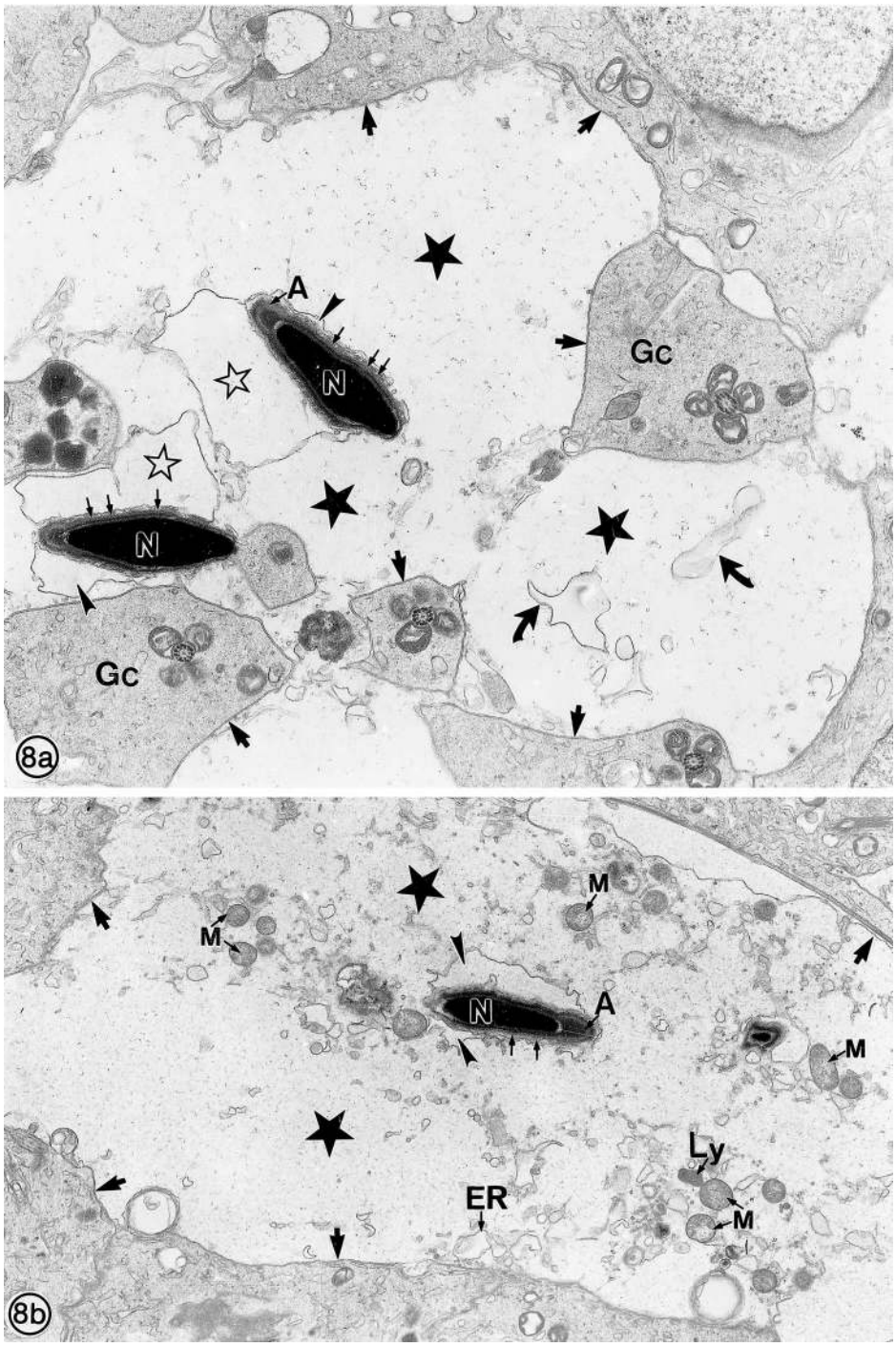

FIG. 8. Apical Sertoli cell processes enveloping the heads of elongating spermatids near the tubular lumen of 6-mo-old FORKO mice. In **a**, an extremely dilated space (solid stars) envelops the heads of elongating spermatids and contains no apparent ground substance or organelles of identifiable nature, aside from several membranous profiles (curved arrows). Such spaces are not territories of the tubular lumen, as they are consistently delimited by a plasma membrane (short arrows). Note that the latter is closely applied to the plasma membrane delimiting the neighboring elongating germ cell cytoplasm (Gc). The ectoplasmic specialization enveloping the spermatid head shows few bundles of filaments (small arrows), while the ER cisternae overlying them (arrowheads) are at times dilated (open stars). In **b**, the grossly dilated Sertoli cell process (solid stars) enveloping the elongating spermatid head contains organelles such as mitochondria (M), lysosomes (Ly), and ER cisternae, embedded in what appears to be a highly diluted ground substance. The plasma membrane of the dilated Sertoli process (short arrows) closely approximates that of the intact germ cell cytoplasm. A, Acrosome. **a**) Original magnification ×10 750; (**b**) original magnification ×8600.

pear to be continuous with the lumen of the tubule, as they were consistently delimited by a plasma membrane (Fig. 8, a and b).

Quantitative Analyses

Quantitative measurements indicated that the mean cross-sectional profile area of seminiferous tubules in FORKO mice was significantly lower compared with wild-type mice at all ages examined (Fig. 9 and Table 1). In addition, both groups showed significant changes in mean profile areas of the tubules as the age of the animals increased (Fig. 9 and Table 1). The mean profile area of tubules in wild-type mice rose by about 5700 μm^2; per tubule from 3 mo and 6 mo and then increased by an additional 14 300 μm^2 per tubule between 6 mo and 12 mo of age (Fig. 9). The mean profile area of tubules in FORKO mice, however, decreased by about 3500 μm^2 per tubule from 3 mo and 6 mo and then increased by 13 900 μm^2 per tubule, roughly the same increment detected for wild-type mice between 6 mo and 12 mo of age (Fig. 9). These within-group changes in cross-sectional profile areas of the seminiferous tubules were significant across all ages (Table 1).

Western Blots

Western blots of testicular extracts from wild-type and FORKO mice probed with the anti-ABP antibody showed the presence of reactive bands, as expected, near 75 kDa. The reactive bands appeared more intense in the extracts

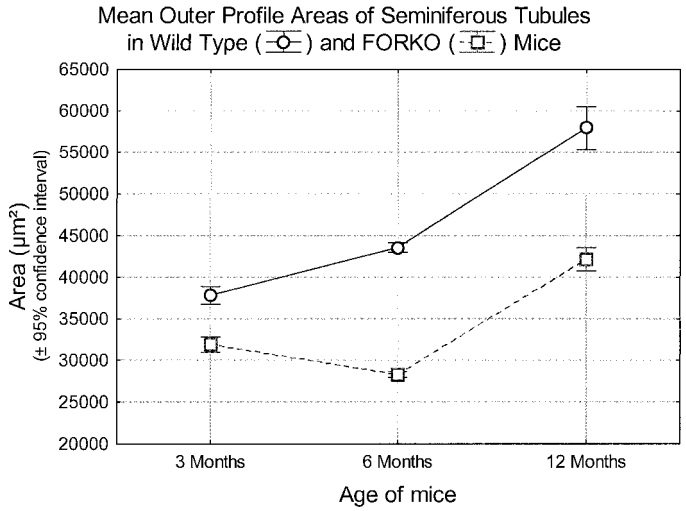

FIG. 9. Mean cross-sectional profile area of seminiferous tubules in wild-type (circles, solid line) and FORKO (squares, dashed line) mice at different ages. The mean profile area of tubules in FORKO mice is significantly less than ($P < 0.05$) the mean profile area of tubules in wild-type mice at all ages. The mean profile area of the tubules also increases markedly between 3 mo and 12 mo of age, and in the same ratio from 6 mo to 12 mo of age, in both groups.

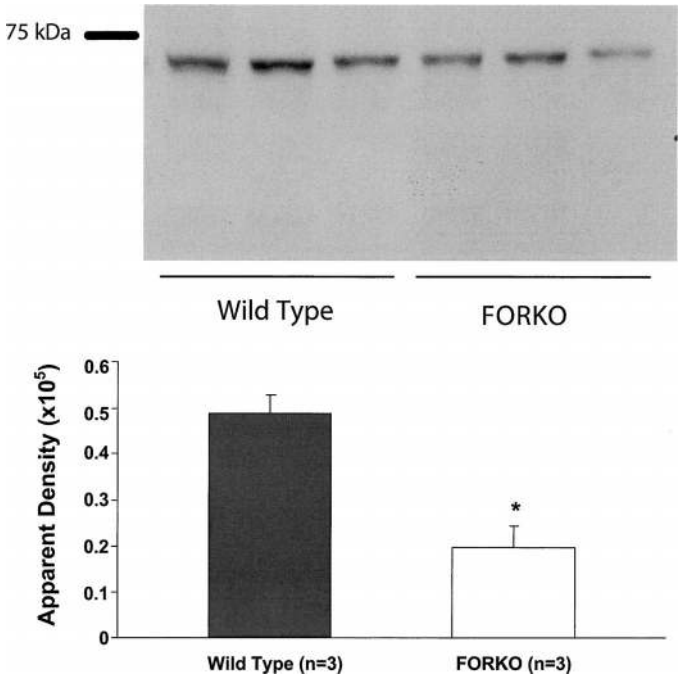

FIG. 10. Western blot of anti-ABP peptide antibody on testicular extracts of 6-mo-old wild-type and FORKO mice (three lanes each from left to right) and corresponding density scan (graph at bottom). A band near 75 kDa, the molecular mass expected for ABP, is seen in all extracts. Average density scans from the three lanes for each group suggest that the amount of ABP protein present in 30 μg whole homogenate of FORKO mice is considerably less than 30 μg of whole homogenate from the wild-type mice. The 30-kDa band seen in all sample lanes is attributable to GST protein that is part of the antigen and also present in the Leydig cells and served as the protein loading control (not shown).

from the wild-type mice compared with the FORKO mice at equivalent total protein loads per lane (Fig. 10; density data). Another set of reactive bands near 30 kDa was also observed in these blots and were caused by anti-GST immunoreactivity simultaneously present in the anti-ABP antibody (the antigen used to elicit the antibody was a recombinant GST-fusion protein) (data not shown). This antigen expressed in the testicular Leydig cells served as the control for equal protein loading in different lanes (data not shown).

DISCUSSION

The most striking aspect of the present study was the finding of large irregularly shaped translucent spaces situated between germ cells in the testis of FORKO mice. For a variety of reasons, it was concluded that these spaces within the epithelium were territories of the Sertoli cell cytoplasm that were highly dilated and filled with fluid. In appropriate planes of section, it was noted that the basal cytoplasm of Sertoli cells at times appeared intact, showing a nucleus and organelles embedded in a finely flocculent ground substance (Fig. 11). These intact areas were confluent with the highly dilated space that extended toward the lumen. The fact that such spaces were always delimited by a plasma membrane indicated that they were of cellular origin. Indeed, such spaces contained membranous profiles of varying sizes and organelles such as mitochondria, ER, and lysosomes characteristic of those normally found in Sertoli cells (Fig. 11). On no occasion were the membrane-bound dilated spaces continuous with the lumen. Furthermore, the epithelium and lumen of the efferent ducts appeared intact, as did that of the epididymis, suggesting that fluid was not backing up into the lumen of seminiferous tubules. In contrast, in estrogen receptor alpha knockout mice, the epithelium of the efferent ducts is affected, resulting in fluid accumulation in the seminiferous tubular lumen and disruption of the epithelium [45, 46]. More apically, the dilated spaces surrounded the heads of elongating spermatids (Fig. 11). Being membrane bound, such spaces corresponded to the cytoplasm of the apical processes of Sertoli cells that are known to envelop the heads of spermatids in various mammals at different stages of the cycle [47, 48]. There was no evidence of dilations of the cytoplasm of any generation of germ cells. Thus, in the absence of the FSH-R, Sertoli cells show dilations of their cytoplasm, with apparent accumulation of fluid and concurrent loss of ground substance (Fig. 11).

For several reasons, we believe that observations on dilated spaces in FORKO testes are real and not artifacts. First, the testes used for EM analyses were always fixed by

TABLE 1. Descriptive statistics (A) and univariate ANOVA tests (B) on $\log_{10}$ trasformed data.

Summary results for outer profile areas (μm^2)		
Group	Age (no.)	Mean ± SD (num. obs.)
Wild type	3	37 822 ± 8815 (245)
	6	43 580 ± 4543 (235)
	12	57 918 ± 17 089 (172)
FORKO	3	31 863 ± 7244 (239)
	6	28 289 ± 2737 (220)
	12	42 179 ± 10 477 (218)

Two-factor univariate ANOVA tests of significance for outer profile areas					
Effect*	SS	Degrees of freedom	MS	*F*	*P*
Treatment	5.4218	1	5.4218	652	0.0000
Age	5.3993	2	2.6996	325	0.0000
Treatment × age	0.6651	2	0.3325	40	0.0000

* Treatment (wild type of FORKO); age (3, 6, or 12 mo.).

cardiac perfusion with either 2.5% or 5% glutaraldehyde. In both cases, the dilated spaces were consistently found in FORKO mice but never in their wild-type counterparts. Second, concurrent perfusions of mice from many other knockout models studied in our laboratory by identical procedures never resulted in dilated spaces of the type seen in the FORKO mice, indicating that these spaces are not related to the fixative or the method used to perfuse FORKO mice [49, 50]. Third, dilated cytoplasmic areas in different generations of germ cells were never observed in the FORKO mice. The dilations were exclusively restricted to cytoplasm of Sertoli cells, suggestive of something specific about the relationship of the knockout to these particular cells. Fourth, in all cases, there were no signs of bloating of the mitochondria, Golgi apparatus, or lysosomes of germ cells or Sertoli cells, perturbations that are commonly seen in poorly fixed immersed testes. Thus, the dilations of the Sertoli cell cytoplasm appear to be a direct consequence of the absence of FSH-R signaling in these cells. The fact that these spaces appear to be filled with fluid, as indicated by the absence of the finely flocculent ground substance seen in wild-type mice (Fig. 11), suggests that FSH-R signaling could potentially regulate water balance in the Sertoli cell.

As Sertoli cells are difficult to visualize in standard fixation and staining preparations, with only their nuclei being prominent, we utilized an antiprosaposin antibody, a specific marker of Sertoli cells, to stain these cells. Prosaposin has been localized to Sertoli cells, irrespective of the stage of the cycle, and in conjunction with immunocytochemistry, the antibody readily stains these cells. In this way, we were able to note that Sertoli cells in FORKO mice showed a radial stellate-shaped distribution around each tubule in a manner similar to that seen in wild-type mice. One point that should be noted is that the dilated appearance of the immersed Bouin-fixed Sertoli cells of FORKO mice was not as readily evident as in vascular-perfused, glutaraldehyde-fixed Epon-embedded tissue. We suspect that the difference is due to the rapid and effective process of cross-linking proteins with glutaraldehyde combined with vascular perfusion that more readily reflects the true status of the tissue.

An interesting observation in FORKO mice was the finding that not all seminiferous tubules appeared affected to the same degree, as only about 60% of tubules present in any random section of testis showed the characteristic dilated phenotype in the cytoplasm of Sertoli cells. In addition, the tubules that were affected usually displayed a semilunar disruption, i.e., only one half of the tubule was affected in a cross-section. Affected tubules were found at all stages of the cycle of the seminiferous epithelium, suggesting that this phenomenon is not stage specific. The quantitative data indicated very clearly that, while focal areas of Sertoli cell cytoplasm appear swollen, this effect does not extend globally to the entire tubule itself, which actually is reduced by 16%, 35%, and 30% in profile area at 3, 6, and 12 mo, respectively in the FORKO mice relative to the wild-type mice. It is unclear at this time if this shrinkage in cross-sectional area of tubules in the knockout animals is caused by a decrease in the number of cells lining the walls of the tubules, a condensation of all cells lining the tubules, or a decrease in internal fluid pressure or amount that normally keeps the tubules in a more expanded state. Our previous study [38] showed that Sertoli cell numbers at 21 days of age are reduced in the absence of FSH-receptors, as compared with wild-type mice, with a concomitant inability to support a full complement of germ cells in the adult [30, 37]. As Sertoli cells normally stop dividing by Day 21, we did not count the number of Sertoli cells in adult FORKO mice in this study; there was no evidence of mitosis of Sertoli cell nuclei at any ages examined in the present investigation.

The finding that some tubules in a cross-section appear normal while others show varying degrees of altered epithelium is apparently not unique to the FORKO testis and has also been reported for other knockout mouse models [49, 51]. While the underlying reasons for such a phenomenon are still not fully understood, several speculations can be advanced. It is possible that the protein(s) regulated by the FSH-R cascade and that are affected in FORKO mice may reside in only some Sertoli cells and not in others. It is also possible that not all Sertoli cells encompassing a given tubule express the FSH receptor, or equal amounts of it, at the same time. Alternately, there may be different subpopulations among Sertoli cells that are functionally different from the others. Thus, one population may be involved more in fluid transport, while another in elevated protein synthesis, and yet another in endocytosis. These types of studies have not been addressed in the various Sertoli cells of a given seminiferous tubule at a given stage of the cycle. Nevertheless, the reason why Sertoli cells have evolved such complex mechanisms of protein regulation is unclear, but the data suggest that the testis has some capacity to maintain itself in part under adverse conditions.

The question also arises as to what mechanism(s) possibly gives rise to the abnormalities found in the cytoplasm of Sertoli cells of FORKO mice. Considering the dilated nature of the cytoplasm, it is likely that these cells, as noted earlier, are accumulating fluid, which would account for the absence of ground substance and the transparent nature of the FORKO Sertoli cytoplasm. Among their many functions, Sertoli cells move water from the interstitial space to the lumen of the seminiferous tubule, where it serves as the vehicle for transporting sperm into the epididymis [12, 13]. This occurs along a standing osmotic gradient created by Na^+K^+/ATPase, which has been localized to the basolateral plasma membranes of Sertoli cells [52, 53]. In early studies, several investigators showed a correlation between increased tubular fluid production and FSH administration [21, 54, 55]. In addition, the onset of tubular fluid production at 20–35 days coincides with a prepubertal rise in FSH [21]. Based on these observations and our findings of a dilated Sertoli cell cytoplasm in FORKO mice, it seems likely that FSH-R regulates water balance in the Sertoli cells. Recent findings reported by Haywood et al. [56] using the hpg mouse model lend support to this hypothesis. These

FIG. 11. Schematic drawing of a portion of the seminiferous epithelium of a wild-type (upper) and FORKO (lower) mouse at 3 mo of age as seen in the electron microscope. In wild-type mice (upper panel), there is a close relationship between Sertoli cells and adjacent spherical and elongating germ cells. The cytoplasm of the Sertoli cell is compact, containing numerous organelles embedded in a finely flocculent ground substance. The thin, attenuated apical Sertoli cell processes (Sp) extend between the elongating spermatids seen near the lumen and contain various organelles. The ectoplasmic specializations (ES, also seen in inset) adhere to the heads of elongating spermatids and are composed of filaments (f) and flattened ER cisternae. The blood testis barrier (BTB) is intact and seen in the basal region of the epithelium. In FORKO mice (lower panel), the Sertoli cell cytoplasm is greatly distended and there is a lack of structural epithelial integrity in areas where abnormalities prevail. Also prominent are large, dilated apical Sertoli cell processes, which encompass elongating spermatids. In such areas, there is an absence of the finely flocculent ground substance, and few organelles are evident amid membra-

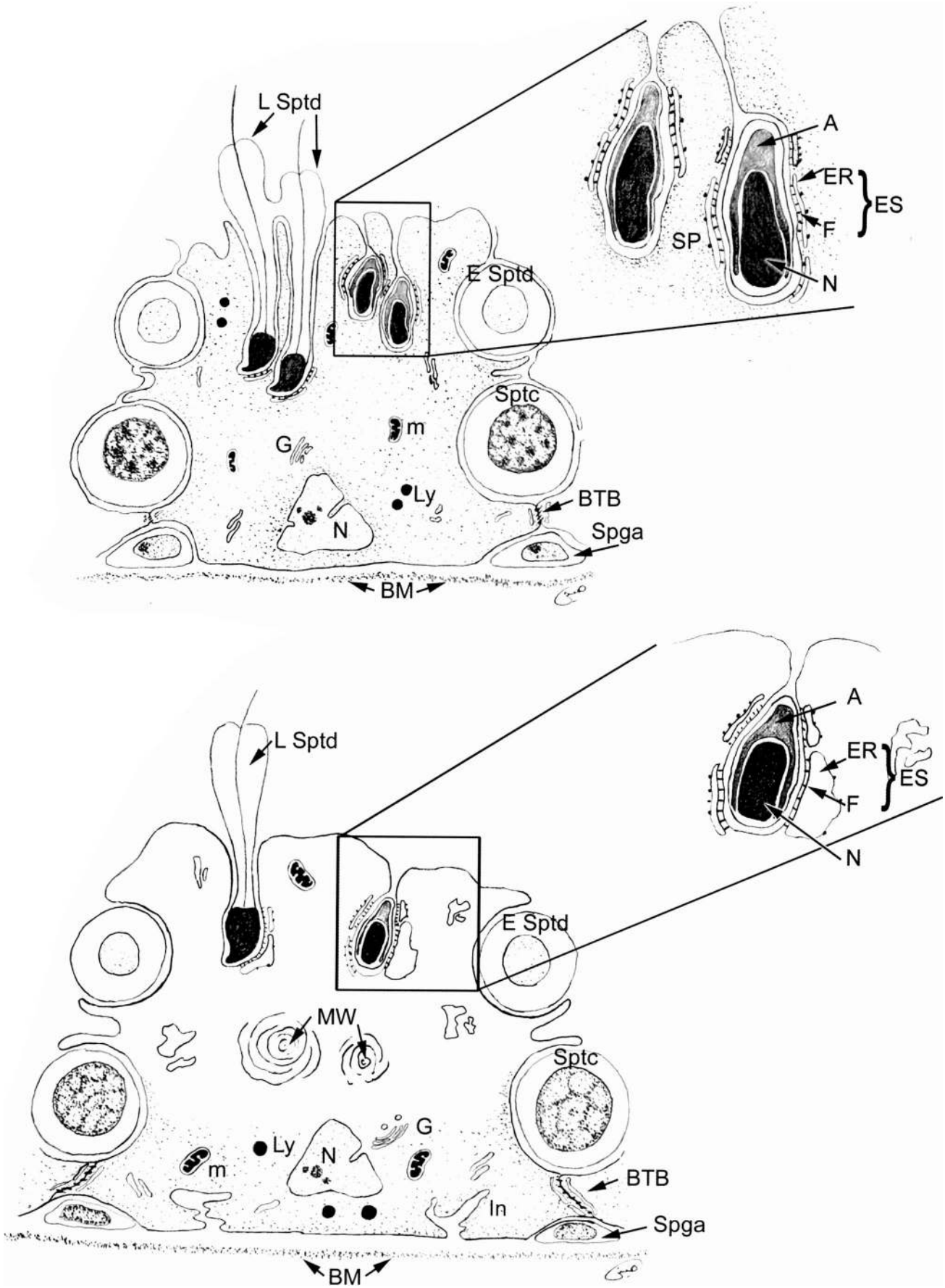

nous whorls (MW) and profiles of varying shapes and sizes. Ectoplasmic specializations (ES, also seen in inset), while apparent, show fewer filaments (f) and occasional dilated ER cisternae. In the basal region, the blood testis barrier (BTB) is present and apparently intact. G, Golgi apparatus; m, mitochondria; Ly, lysosomes; In, invagination; A, acrosome; N, nucleus of Sertoli cell; Spct, spermatocyte; Spga, spermatogonia; LSptd, late spermatid; ESptd, elongating spermatid. Illustration by Haitham Badran.

mice lack gonadotropins, and constitutively express a mutated FSH-R, showing increased levels of tubular fluid secretion resulting from overactive FSH-R signaling.

Recently, the expression and immunolocalization of several water channel proteins, aquaporins (AQPs), have been described in the testis of rats [14, 15, 57]. AQPs are essential for regulating water homeostasis and for providing sustained and rapid movement of fluid across a tightly sealed epithelium with minimal activation costs [58, 59]. There are at least 11 different members of the AQP family [16], with several containing cAMP motifs and CREB binding regions that regulate their transcription [17–20]. A systematic effort to localize AQPs in the testis of these mice would be required to fully understand hormonal/receptor regulation of these channels.

Considering the abnormality seen in the Sertoli cell cytoplasm, the question arises whether it is possible that such cells degenerate with time, thus compromising the seminiferous epithelium. In fact, at no time did we observe pyknosis of Sertoli cell nuclei, degeneration of their organelles, or evidence of apoptotic figures in the seminiferous epithelium. In addition, the basal Sertoli cell cytoplasm and junctional complexes between adjacent Sertoli cells appeared intact. Furthermore, the absence of an increased number of macrophages or neutrophils in the interstitial space of the testis of FORKO mice suggests that there is no leakage of substances from the epithelium as a result of the swelling of the Sertoli cell cytoplasm or complete breakdown of the blood/testis barrier. On the other hand, the ectoplasmic specializations enveloping the heads of spermatids (steps 9–16) appeared compromised. The bundles of filaments were not extensively distributed and the ER cisternae of these specializations were at times dilated (Fig. 11), unlike relationships normally seen in wild-type mice [60]. However, the adhesive function of these structures appeared to be maintained, as spermatids were still closely associated with the apical Sertoli cell processes despite the fact that the latter were grossly dilated.

One of the major proteins regulated by FSH and secreted by Sertoli cells into the lumen is ABP [22, 26]. In the present study, LM immunocytochemistry revealed that ABP was expressed intensely in Sertoli cells, but the reaction was dramatically reduced in FORKO mice, a finding confirmed by the Western blot analyses. This may be due to the dilated nature of the Sertoli cell cytoplasm and its effect on secretory organelles, such as the ER and Golgi apparatus, which appeared to be less prominent than in wild-type mice and which would affect secretion. However, it is equally possible that regulation is affected at the mRNA level. As ABP is a major carrier protein delivering high concentrations of testosterone to the epididymis [61], it is also likely that the epididymis, an androgen-dependent tissue, could be compromised in FORKO mice [30, 38]. Altered epididymal functions could result in many sperm aberrations that we have previously described in FORKO mice (30, 37, 38) accounting for their reduction in fertility. We are presently investigating the epididymis with respect to its structure and functions of its epithelial cells and sperm motility parameters in FORKO mice. Thus, aside from the apparent effect on water balance in Sertoli cells, FSH-R signaling also appears to be a main player in regulating ABP production, which may have an indirect effect on epididymal functions and sperm motility.

ACKNOWLEDGMENTS

We thank Ms. Jeannie Mui for her excellent EM technical assistance and Dr. Elaine Davis for help with the Western blots. We also thank Dr. G.L. Hammond, University of Western Ontario, London, Canada, for donating the anti-ABP antibody and Dr. C.R. Morales from McGill University for providing the antiprosaposin antibody. The assistance of Sarah Torabi and Heather Smith in obtaining quantitative data is also gratefully acknowledged.

REFERENCES

1. Simoni M, Gromoll J, Nieschlag E. The follicle stimulating hormone receptor. Biochemistry, molecular biology, physiology and pathophysiology. Endocr Rev 1997; 18:739–773.
2. Sairam MR, Jiang LG, Yarney TA, Khan H. Alternate splicing converts the G-protein coupled follitropin receptor into a growth factor type I receptor: implications for pleiotropic actions of the hormone. Mol Reprod Dev 1997; 48:471–479.
3. Babu PS, Krishnamurthy H, Chedrese PJ, Sairam MR. Activation of extracellular regulated kinase pathways in ovarian granulosa cells by the novel growth factor type I follicle-stimulating hormone receptor: role in hormone signaling and cell proliferation. J Biol Chem 2000; 275:27615–27626.
4. Parvinen M. Cyclic function of Sertoli cells. In: Russell LD, Griswold MD (eds.), The Sertoli Cell. Clearwater, FL: Cache River Press; 1993: 331–347.
5. Parvinen M, Marana R, Robertson DM, Hansson V, Ritzén EM. Functional cycle of rat Sertoli cells: differential binding and action of follicle stimulating hormone at various stages of the spermatogenic cycle. In: Steinberger A, Steinberger E (eds.), Testicular Development, Structure and Function. New York: Raven Press; 1980:425–432.
6. Kangasniemi M, Kaipia A, Mali P, Toppari J, Huhtaniemi I, Parvinen M. Modulation of basal and FSH-stimulated cyclic AMP production in rat seminiferous tubules staged by an improved transillumination technique. Anat Rec 1990; 227:62–76.
7. Waeber G, Meyer TE, LeSieur M, Hermann HL, Gérard N, Habener JF. Developmental stage-specific expression of cyclic adenosine 3′,5′-monophosphate response element-binding protein CREB during spermatogenesis involves alternative exon splicing. Mol Endocrinol 1991; 5:1418–1430.
8. Fawcett DW. Ultrastructure and function of the Sertoli cell. In: Hamilton DW, Greep RO (eds.), Handbook of Physiology, Section 7, Endocrinology, vol. 5. Male Reproductive System. Baltimore: Williams and Wilkins. The American Physiological Society (Washington, DC); 1975:21–55.
9. Griswold MD. Protein secretion by Sertoli cells: general considerations. In: Russell LD, Griswold MD (eds.), The Sertoli Cell. Clearwater, FL: Cache River Press; 1993:195–200.
10. Russell LD. Role in spermiation. In: Russell LD, Griswold MD (eds.), The Sertoli Cell. Clearwater, FL: Cache River Press; 1993:269–303.
11. Hermo L, Oko R, Morales C. Secretion and endocytosis in the male reproductive tract: a role in sperm maturation. Int Rev Cytol 1994; 154:105–189.
12. Setchell BP, Scott TW, Voglmayr JK, Waites GMH. Characteristics of spermatozoa and the fluid which transports them into the epididymis. Biol Reprod 1969; 1(suppl):40–66.
13. Hinton BT, Setchell BP. Fluid secretion and movement. In: Russell LD, Griswold MD (eds.), The Sertoli Cell. Clearwater, FL: Cache River Press; 1993:249–268.
14. Tani T, Koyama Y, Nihei K, Hatakeyama S, Ohshiro K, Yoshida Y, Yaoita E, Sakai Y, Hatakeyama K, Yamamoto T. Immunolocalization of aquaporin-8 in rat digestive organs and testis. Arch Histol Cytol 2001; 64:159–168.
15. Badran HH, Hermo L. Expression and regulation of aquaporins 1, 8, and 9 in the testis, efferent ducts, and epididymis of adult rats and during postnatal development. J Androl 2002; 23:358–373.
16. Hermo L, Robaire B. Epididymal cell types and their functions. In: Robaire B, Hinton BT (eds.), The Epididymis: From Molecules to Clinical Practice. New York: Kluwer Academic/Plenum Publishers; 2002:81–102.
17. Yang F, Kawedia JD, Menon AG. Cyclic amp regulates aquaporin 5 expression at both transcriptional and post-transcriptional levels through a protein kinase A pathway. J Biol Chem 2003; 278:32173–32180.
18. Wang S, Chen J, Au KT, Ross MG. Expression of aquaporin 8 and its upregulation by cyclic adenosine monophosphate in human WISH cells. Am J Obstet Gynecol 2003; 188:997–1001.
19. Garcia F, Kierbel A, Larocca MC, Grandilone SA, Splinter P, LaRusso NF, Marinelli RA. The water channel aquaporin-8 is mainly intracel-

lular in rat hepatocytes, and its plasma membrane insertion is stimulated by cyclic-AMP. J Biol Chem 2001; 276:12147–12152.
20. Hozawa S, Holtzman EJ, Ausiello DA. cAMP motifs regulating transcription in the aquaporin 2 gene. Am J Physiol 1996; 270:C1695–C1702.
21. Jegou B, Le Gac F, de Kretser DM. Seminiferous tubule fluid and interstitial fluid production. I. Effects of age and hormonal regulation in immature rats. Biol Reprod 1982; 27:590–595.
22. Munell F, Suárez-Quian CA, Selva DM, Tirado OM, Reventós J. Androgen-binding protein and reproduction: where do we stand? J Androl 2002; 23:598–609.
23. French FS, Ritzén EM. A high affinity androgen-binding protein (ABP) in rat testis: evidence for secretion into efferent duct fluid and absorption by epididymis. Endocrinology 1973; 93:88–95.
24. Danzo BJ, Eller BC, Orgebin-Crist M-C. Studies on the site of origin of the androgen binding protein present in epididymal cytosol from mature intact rabbits. Steroids 1974; 24:107–122.
25. Joseph DR, Hall SH, Conti M, French FS. The gene structure of rat androgen-binding protein: identification of potential regulatory deoxyribonucleic acid elements of a follicle-stimulating-hormone regulated protein. Mol Endocrinol 1988; 2:3–13.
26. Hansson V, Weddington SC, Naess O, Attramandal A, French FS, Kotite N, Nayfeh SN. Testicular androgen binding protein (ABP)—a parameter of Sertoli cell secretory function. Curr Top Mol Endocrinol 1975; 2:323–336.
27. Esteban C, Gerard A, Larriba S, Toràn N, Gerard H, Reventós J. Sertoli cell-specific expression of rat androgen-binding protein in transgenic mice: effects on somatic cell lineages. Mol Cell Endocrinol 1997; 132:127–136.
28. Larriba S, Esteban C, Toràn N, Gerard A, Audi L, Gerard H, Reventós J. Androgen binding protein is tissue-specifically expressed and biologically active in transgenic mice. J Steroid Biochem Mol Biol 1995; 53:573–578.
29. Griswold MD. Actions of FSH on mammalian Sertoli cells. In: Russell LD, Griswold MD (eds.), The Sertoli Cell. Clearwater, FL: Cache River Press; 1993:494–508.
30. Krishnamurthy H, Danilovich N, Morales CR, Sairam MR. Qualitative and quantitative decline in spermatogenesis of the follicle-stimulating hormone receptor knockout (FORKO) mouse. Biol Reprod 2000; 62: 1146–1159.
31. Sairam MR, Krishnamurthy H. The role of follicle-stimulating hormone in spermatogenesis: lessons from knockout animal models. Arch Med Res 2001; 32:601–608.
32. Layman LC, McDonough PG. Mutations of follicle stimulating hormone-β and its receptor in human and mouse: genotype/phenotype. Mol Cell Endocrinol 2000; 161:9–17.
33. Phillip M, Arbelle JE, Segev Y, Parvari R. Male hypogonadism due to a mutation in the gene for the β-subunit of follicle stimulating hormone. N Engl J Med 1998; 338:1729–1732.
34. Lindstedt G, Nystrom E, Matthews C, Ernest I, Janson PO, Chatterjee K. Follitropin (FSH) deficiency in an infertile male due to FSH beta gene mutation. A syndrome of normal puberty and virilization but underdeveloped testicles with azoospermia, low FSH but high lutropin and normal serum testosterone concentrations. Clin Chem Lab Med 1998; 36:663–665.
35. Kumar TR, Wang Y, Lu N, Matzuk MM. Follicle stimulating hormone is required for ovarian follicle maturation but not male fertility. Nat Genet 1997; 15:201–204.
36. Tapanainen JS, Aittomaki K, Min J, Vaskivuo T, Huhtaniemi IT. Men homozygous for an inactivating mutation of the follicle-stimulating hormone (FSH) receptor gene present variable suppression of spermatogenesis and fertility. Nat Genet 1997; 15:205–206.
37. Dierich A, Sairam MR, Monaco L, Fimia GM, Gansmuller A, LeMeur M, Sassone-Corsi P. Impairing follicle-stimulating hormone (FSH) signaling in vivo: targeted disruption of the FSH-receptor leads to aberrant gametogenesis and hormonal imbalance. Proc Natl Acad Sci U S A 1998; 95:13612–13617.
38. Krishnamurthy H, Babu PS, Morales CR, Sairam MR. Delay in sexual maturity of the follicle-stimulating hormone receptor knockout male mouse. Biol Reprod 2001; 65:522–531.
39. Krishnamurthy H, Kats R, Danilovich N, Javeshghani D, Sairam MR. Intercellular communication between Sertoli cells and Leydig cells in the absence of follicle-stimulating hormone-receptor signaling. Biol Reprod 2001; 65:1201–1207.
40. Danilovich N, Babu PS, Xing W, Gerdes M, Krishnamurthy H, Sairam MR. Estrogen deficiency, obesity and skeletal abnormalities in follicle stimulating hormone receptor knockout (FORKO) female mouse. Endocrinology 2000; 141:4295–4308.
41. Morales CR, Zhao Q, El-Alfy M, Suzuki K. Targeted disruption of the mouse prosaposin gene affects the development of the prostate gland and other male reproductive organs. J Androl 2000; 21:765–775.
42. Lee WM, Wong AS, Tu AW, Cheung CH, Li JC, Hammond GL. Rabbit sex hormone binding globulin: primary structure, tissue expression, and structure/function analyses by expression in *Escherichia coli*. J Endocrinol 1997; 153:373–384.
43. Danilovich N, Roy I, Sairam MR. Ovarian pathology and high incidence of sex cord tumors in follitropin receptor knockout (FORKO) mice. Endocrinology 2001; 142:3673–3684.
44. Papp S, Robaire B, Hermo L. Immunocytochemical localization of the Ya, Yc, Yb1, and Yb2 subunits of glutathione S-transferase in the testis and epididymis of adult rats. Microsc Res Tech 1995; 30:1–23.
45. Hess RA, Zhou Q, Nie R. The role of estrogens in the endocrine and paracrine regulation of the efferent ductules, epididymis and vas deferens. In: Robaire B, Hinton BT (eds.), The Epididymis. From Molecules to Clinical Practice. New York: Kluwer Academic/Plenum Press Publishers; 2002:317–337.
46. Hess RA, Bunick D, Lee KH, Bahr J, Taylor JA, Korach KS, Lubahn DB. A role for oestrogens in the male reproductive tract. Nature 1997; 390:509–512.
47. Clermont Y, McCoshen J, Hermo L. Evolution of the endoplasmic reticulum in the Sertoli cell cytoplasm encapsulating the heads of late spermatids in the rat. Anat Rec 1980; 196:83–99.
48. Russell LD. Morphological and functional evidence for Sertoli-germ cell relationships. In: Russell LD, Griswold MD (eds.), The Sertoli Cell. Clearwater, FL: Cache River Press; 1993:365–390.
49. Chung S, Wang SP, Pan L, Mitchell G, Trasler J, Hermo L. Infertility and testicular defects in hormone-sensitive lipase-deficient mice. Endocrinology 2001; 142:4272–4281.
50. Korah N, Smith CE, D'Azzo A, El-Alfy M, Hermo L. Increase in macrophages in the testis of cathepsin A deficient mice suggests an important role for these cells in the interstitial space of this tissue. Mol Reprod Dev 2003; 64:302–320.
51. Rao DS, Chang JC, Kumar PD, Mizukami I, Smithson GM, Bradley SV, Parlow AF, Ross TS. Huntingtin interactin protein 1 is a clathrin coat binding protein required for differentiation of late spermatogenic progenitors. Mol Cell Biol 2001; 21:7796–7806.
52. Barham SS, Berlin JD, Brackeen RD. The fine structural localization of testicular phosphatases in man: the control testis. Cell Tissue Res 1976; 166:497–510.
53. Gravis CJ, Yates RD, Chen IL. Light and electron microscopic localization of ATPase in normal and degenerating testes of Syrian hamsters. Am J Anat 1976; 147:419–432.
54. Murphy HD. Sertoli cell stimulation following intratesticular injections of FSH in the hypophysectomized rat. Proc Soc Exp Biol Med 1965; 118:1202–1205.
55. Setchell BP, Duggan MC, Ewans RW. The effect of gonadotrophins on fluid secretion and sperm production by the rat and hamster testis. J Endocrinol 1973; 56:27–36.
56. Haywood M, Tymchenko N, Spaliviero J, Koch A, Jimenez M, Gromoll J, Simoni M, Nordhoff V, Handelsman DJ, Allan CM. An activated human follicle-stimulating hormone (FSH) receptor stimulates FSH-like activity in gonadotropin-deficient transgenic mice. Mol Endocrinol 2002; 16:2582–2591.
57. Verkman AS, Mitra AK. Structure and function of aquaporin water channels. Am J Physiol Renal Physiol 2000; 278:F13–28.
58. Preston GM, Agre P. Molecular cloning of the red cell integral protein of Mr 28000: a member of an ancient channel family. Proc Natl Acad Sci U S A 1991; 88:11110–11114.
59. Agre P, Preston GM, Smith BL, Jung JS, Raina S, Moon C, Guggino WB, Nielsen S. Aquaporin CHIP: the archetypal molecular water channel. Am J Physiol 1993; 34:F463–F476.
60. Vogl AW, Pfeiffer DC, Redenbach DM, Grove BD. Sertoli cell cytoskeleton. In: Russell LD, Griswold MD (eds.), The Sertoli Cell. Clearwater, FL: Cache River Press; 1993:39–86.
61. Turner TT. Necessity's potion: inorganic ions and small organic molecules in the epididymal lumen. In: Robaire B, Hinton BT (eds.), The Epididymis: From Molecules to Clinical Practice. New York: Kluwer Academic/Plenum Publishers; 2002:131–150.